

1 *Type of the Paper (Review)*

## 2 **Title: Role of PhaC type I and type II enzymes during** 3 **PHA biosynthesis.**

4 **Valeria Mezzolla,<sup>1</sup> Oscar Fernando D'Urso<sup>2</sup> and Palmiro Poltronieri <sup>3\*</sup>**

5 <sup>1</sup> Bioesplora, Department of Biological and Environmental Science and Technologies, Ecotekne, Lecce;

6 [Bioesplora@gmail.com](mailto:Bioesplora@gmail.com); [valeria.mezzolla@gmail.com](mailto:valeria.mezzolla@gmail.com);

7 <sup>2</sup> Bioesplora, Department of Biological and Environmental Science and Technologies, Ecotekne, Lecce;

8 [doscarferna@gmail.com](mailto:doscarferna@gmail.com)

9 <sup>3</sup> Institute of Sciences of Food Productions (ISPA-CNR), via Monteroni km 7, 73100 Lecce, Italy;

10 \* Correspondence: [palmiro.poltronieri@ispa.cnr.it](mailto:palmiro.poltronieri@ispa.cnr.it); Tel.: +39-0832-422609

11

12

13 **Abstract:** PHA synthases (PhaC) are grouped into four classes based on the kinetics and  
14 mechanisms of reaction. The grouping of PhaC enzymes into four classes is dependent on substrate  
15 specificity, according to the preference in forming short chain length (scl) or medium chain length  
16 (mcl) polymers: class I, class III, and class IV produce scl-PHAs depending on propionate, butyrate,  
17 valerate and hexanoate precursors, while class II phaC synthesize mcl-PHAs based on the alkane (C6  
18 to C14) precursors.

19 PHA synthases of class I, in particular PhaC<sub>Cs</sub> from *Chromobacterium* USM2 and PhaC<sub>Cn</sub>/RePhaC1  
20 from *Cupriavidus necator*/R. *eutropha*, have been analysed and the crystal structures of the C-domains  
21 have been determined. PhaC<sub>Cn</sub>/RePhaC1 was also studied by small angle X-ray scattering (SAXS)  
22 analysis. Models have been proposed for dimerization, catalysis mechanism, substrate recognition  
23 and affinity, product formation and product egress route. The assays based on amino acid  
24 substitution by mutagenesis have been useful to validate the hypothesis on the role of amino acids in  
25 catalysis and in accommodation of bulky substrates, for the synthesis of PHB co-polymers and  
26 medium chain length-PHA polymers with optimized chemical properties.

27 **Keywords:** PhaC synthase, classification, dimerization, substrate binding, exit cavity, C3-C14  
28 alkanes, polymer composition.

29

---

### 30 **1. Introduction**

31 Polyhydroxyalkanoates (PHAs) are biodegradable polyesters produced in several Gram-negative  
32 and Gram-positive bacteria, in archea and cyanobacteria [1-8]. PHAs are polymers containing  
33 various alkanes, such as 3-hydroxy propionate (3HP), butyrate (3HB), valerate (3HV), hexanoate  
34 (3HHx), heptanoate (3HHp), octanoate (3HO), nonanoate (3HN), decanoate (3HD), dodecanoate  
35 (3HDD), in addition to 4-hydroxybutyrate (4HB) or 5-hydroxyvalerate (5HV), and produced  
36 through the availability of the corresponding CoA thioester substrates [9-14].

37 PhaC synthases, the polymerizing enzymes, are grouped into four classes based on substrate  
38 specificity, and the preference in forming short chain length (scl-) or medium chain length (mcl-)  
39 polymers: class I, class III, and class IV produce principally scl-PHAs, while class II phaC synthesize  
40 mcl-PHAs [7, 15].

41 The PHA biosynthesis genes include: *PhaPs*, genes coding for Phasins, the granule assembling  
42 proteins, *PhaM*, encoding the activator and accelerator of the catalytic activity of PHA synthase,  
43 encoded by *PhaC*; *phaA*, encoding the acetoacetyl-CoA  $\beta$ -thiolase, *phbB* coding for the

44 acetoacetyl-CoA reductase, *phaG*, coding for 3-hydroxyacyl-carrier protein-CoA transferase, *phaJ*,  
45 encoding the enoyl-CoA hydratase, and *PhaZ*, encoding the PHA depolymerising enzyme.  
46 PhaC proteins possess the so called lipase box, G-X-S-X-G, and a secondary structure containing the  
47  $\alpha/\beta$  hydrolase fold, a characteristic succession of alpha helices and beta strands, typical of lipases. In  
48 PhaC enzymes, the lipase box has the conserved sequence G-G/S-X-C-X-G/A-G, renamed the PhaC  
49 box consensus sequence. The Cys in the lipase box-like sequence is the catalytic amino acid, forming  
50 the covalently bond intermediate, Cys-S-H3B [7, 16].

51 PHA synthase activity is based on the catalytic triad C-H-D, cysteine, histidine, aspartate, also  
52 responsible for catalysis in lipases (S-H-D). In the catalytic triad, the negatively charged Asp<sup>447</sup> in  
53 PhaC<sub>S</sub> from *Chromobacterium* spp. [17, 18] and Asp<sup>480</sup> in PhaC<sub>N</sub> from *Cupriavidus necator* [19, 20]  
54 assist to enhance the basicity of His<sup>477</sup> and His<sup>508</sup>, respectively, by formation of a direct hydrogen  
55 bond. Previous reports suggest that the Asp residue of the triad acts as a general base catalyst to  
56 accelerate deprotonation of the 3-hydroxyl group of HB in the step involving elongation of the PHA  
57 product.

58 PHA synthases are grouped into four classes based on the kinetics and mechanism of reaction. The  
59 grouping of PhaC enzymes into each class is dependent on the structure of the PhaC, alone or in  
60 association to other subunits, and the substrate specificity: class I, class III, and class IV produce  
61 scl-polymers depending on propionate (3HP), butyrate (3HB, 4HB), valerate (HV) and hexanoate  
62 (HH) precursors (C3 to C6 carbons), while class II phaC enzymes synthesize mcl-polymers  
63 depending on hexanoate (3HH), heptanoate (3HHp), octanoate (3HO), decanoate (3HD),  
64 undecanoate (3HUD), dodecanoate (3HDD) (C6 to C12), and availability of the corresponding CoA  
65 thioester substrates, originating from three different metabolic pathways [9, 10, 20].

66 While some bacterial species produce mainly 3HB polymers, other species can synthesize various  
67 PHAs, depending on availability of intermediate precursors [1, 3, 9]. The structure and properties of  
68 the polymers are affected by the monomers that are incorporated. PHAs can be molded into films  
69 and hollow bodies. Polyhydroxybutyrate (PHB) is brittle, fragile, and stiff, with low elongation  
70 ability, and a break point below 15%. The incorporation of 3-hydroxyvalerate or other co-monomers  
71 can decrease the brittleness of PHB. The thermal, rheological and barrier properties of PHAs show  
72 good application potential in thermoplastic materials. The synthesis of copolymers is a frequent  
73 strategy to improve the properties of PHAs, to improve the plastics flexibility and lower the glass  
74 transition temperature (T<sub>g</sub>) and the melting temperature (T<sub>m</sub>) [21]. P3HB-4HB polymers and  
75 conventional thermoplastic used for packaging show high tensile strength and higher elongation at  
76 break. HBV-containing mcl-PHAs are elastic, have low melting point, a relatively low degree of  
77 crystallinity, and with various tensile strength. PHB copolymer containing 3-hydroxyvalerate unit  
78 P(3HB-co-3HV) has been developed with improved mechanical properties. To this aim, either  
79 optimization of substrate availability (feedstock, successive addition of precursors), and efficiency  
80 of enzymes, through genetic engineering and selection of PHA synthases, have been applied.

81

## 82 **Class I and class II PHA synthases**

83 Classes I and II PHA synthases are formed by a single protein (PhaC), of about 60 kDa.

84 In class I, the active PhaC enzyme is a dimer, with catalytic (CAT) domains facing each other, with  
85 N-domains making direct contacts, sustaining protein interaction and dimerization. It was  
86 hypothesized that a partially folded catalytic domain is partially occupied by the lid and cat domain  
87 secondary structure, that change their conformation in presence of activation factors, to open the  
88 catalytic domain and to allocate the 3HB-CoA in its binding site (Chek et al., 2017).

89 PhaC sequences differ in their length. In *Cupriavidus necator* (formerly *Ralstonia eutropha*) the class I  
90 enzyme PhaC<sub>Cn</sub>/RePhaC, the sequence is composed of a 191 amino acids N-terminal domain  
91 proteolytically cleaved after arginine, and a C-domain, containing the catalytic site, composed of 398  
92 amino acids, for a total of 589 residues (Figure 1). In *C. necator*, PhaC<sub>Cn</sub> contains Cys<sub>319</sub>, Asp<sub>480</sub> and  
93 His<sub>508</sub>, located between the beta 6 and alpha 3 turn, the beta 10 and alpha 7 turn, and at the end of the  
94 beta 11 strand, respectively. In the between of Cys<sub>319</sub> and Asp<sub>480</sub> is located the D-loop and the  
95 helix-turn-helix motif (HTH), formed by  $\alpha 4$ ,  $\alpha 5$ ,  $\alpha 6$ , and  $\beta 7$ - $\beta 8$  stretches [18, 19]. (Wittenborn et al.  
96 ,2016, Kim et al., 2017a). PhaC<sub>Cn</sub>/RePhaC1 was also studied by small angle X-ray scattering (SAXS)  
97 analysis that confirmed the previous findings on the protein assembled as a dimer [22].

98 The PhaC synthase from *Chromobacterium* spp., phaC<sub>Cs</sub>, was extensively studied [16, 17]. PhaC<sub>Cs</sub> has a  
99 peculiarity of utilization of 3HB, 3HV, and 3HH, producing scl-PHA polymers with mixed  
100 composition, with ability to incorporate C5 and C6 alkanes into the PHA polymer. PhaC<sub>Cs</sub> was found  
101 highly active, with fast polymerization rate [17]. PhaC<sub>Cs</sub> is shorter in length (for about 29 amino  
102 acids) in respect to PhaC<sub>Cn</sub> and this produces differences in numbering of amino acids. PhaC<sub>Cs</sub>  
103 structure has a substrate-binding site hidden by a partially disordered protein domain, the CAP  
104 domain [16, 17]. Cysteine<sub>291</sub>, at the end of the  $\beta 6$  sheet, is followed by the CAP domain, containing  
105 the LID structure, that close the accessibility of the substrate access pocket. The  $\beta$  sheets in the CAP  
106 domain have been renumbered with Greek letters in the PhaC<sub>Cs</sub> sequence. Thus, from the N-terminal  
107 sequence, up to the  $\beta 6$ - $\alpha 3$  turn, the two PHA synthases conserve the same numbering in their  
108 secondary structures, but the successive  $\alpha$ - $\beta$  turns are differently numbered. In PhaC<sub>Cs</sub>, the core  
109 subdomain contains six  $\beta$ -strands ( $\beta 8$  to  $\beta 13$ ) and four  $\alpha$ -helices ( $\alpha 4$  to  $\alpha 7$ ), whose number does not  
110 correspond to those in the PhaC<sub>Cn</sub>-CAT structure.

111 In PhaC<sub>Cs</sub> the catalytic triad is composed of Cys<sub>291</sub>, His<sub>477</sub> (located after the  $\beta 9$  sheet, in respect to the  
112  $\beta 11$  sheet in PhaC<sub>Cn</sub>) and Asp<sub>447</sub> (located at the turn formed by  $\beta 8$  strand and  $\alpha 4$  helix, the  $\beta 8$ - $\alpha 4$  fold,  
113 in respect to the  $\beta 10$ - $\alpha 7$  fold in PhaC<sub>Cn</sub>).

114 In other species, such as *Delftia acidovorans* (previously *Comamonas acidovorans*) the PHA synthase  
115 contains a large insert of 40 amino acid residues shown to improve the specific activity of the  
116 enzyme, located in the  $\alpha/\beta$  hydrolase fold, following the catalytic cysteine after the  $\beta 6$  turn [25].

117 *Aeromonas* spp., such as *A. caviae*, *A. hydrophila*, and *A. punctata*, possess PhaC enzymes belonging to  
118 class I. The enzyme PhaC<sub>Cc</sub> from *Caulobacter crescentus* (*C. vibrioides*) [26], displayed to accommodate  
119 alkanes with various alkyl side-chain length.

120 Class II phaC synthases have been extensively studied, and are widely distributed in bacteria: in  
121 *Pseudomonas* spp. (*P. putida*, *P. mendocina*, *P. oleovorans*, *P. campisalis*; *P. stutzeri*) there are two phaC  
122 genes, of which PhaC1 is the active enzyme under physiological conditions. PhaC synthases have  
123 been reported in *Halomonas* spp., such as *H. campisalis*, *Halomonas* sp. O-1 and *Halomonas elongata*  
124 DSM2581 [27], and in *P. stutzeri*, that can be exploited in polymerization of mcl-PHAs [28]. There are  
125 two PHA synthases, PhaC1 and PhaC2, in *P. oleovorans*, of which PhaC2 has a higher affinity for  
126 3-hydroxyhexanoate (3HH) monomers.

127 Class II phaC enzymes differ from PhaC<sub>Cn</sub>, as prototype of class I PHA synthases, for about 28 amino  
128 acids, reaching the C-terminal (1-559) with about 30 amino acids shorter sequence. The catalytic triad  
129 has been renumbered as Cys<sub>296</sub>, Asp<sub>452</sub>, His<sub>453</sub> and His<sub>480</sub> in *Pseudomonas* spp., prototype for Class II  
130 PHA synthases.

131

### 132 **Class III and Class IV PHA synthases**

133 Class III PHA synthases are made of two subunits, namely, a catalytic subunit PhaC (40–53  
134 kDa) and a second subunit PhaE (ranging from 20 to 40 kDa), which form the PhaEC complex, in  
135 which the PhaE subunit is necessary for PHA polymerization. Class III phaC are structured as  
136 tetramers, such as phaEC from *Allochromatium vinosum*, (with catalytic triad Cys<sub>149</sub>, Asp<sub>302</sub>, His<sub>331</sub>),  
137 whose enzyme activity has been studied using substrate analogs [15]. The authors performed  
138 molecular docking and *in silico* studies, that are in agreement with the crystal structure of synthases  
139 available [15], based on homology models built using CPHmodels3.0, SWISS-MODEL and  
140 I-TASSER, performing structure-guided sequence profiles. The results of their analysis, referring to  
141 PhaC<sub>n</sub> and PhaC class III from *Allochromatium vinosum*, describe the presence of an active site of  
142 cysteine, that is buried in a pocket: the authors, by comparison with other enzymes with known  
143 crystal structure (lipases), postulated the presence of the substrate entrance and product exit  
144 channels [15].

145 There is also an Archaeal type, PhaC class IIIA: this group is represented by *Haloarcula marismortui*.  
146 Archaea present good perspectives of exploitation for polymer production, given by the easiness of  
147 PHB extraction.

148 Class IV PHA synthases from *Bacillus* spp. are composed of a catalytic subunit PhaC (41.5 kDa) and a  
149 PhaR (22 kDa) subunit, similarly to class III synthases composed of phaE and phaC units. Class IV  
150 PHA synthases are classified as *B. megaterium* type (IV<sub>m</sub>) [23], *Bacillus cereus* type (IV<sub>c</sub>) [22], and *B.*  
151 *bataviensis* type (IV<sub>b</sub>), with 33% homology to the other phaC sequences [5]. In *E. coli* expressing  
152 PhaRC from *B. cereus* YB-4, the biosynthesized PHA undergoes synthase-catalyzed alcoholic  
153 cleavage using endogenous and exogenous alcohols. This alcoholysis is thought to be shared among  
154 class IV synthases, and this reaction is useful for regulation of PHA molecular weight and for  
155 modification of the PHA carboxy terminus.

156 The catalytic cysteine in the active site is C<sub>151</sub> in *B. cereus*, and C<sub>147</sub> in *B. megaterium* type IV enzymes.  
157 As shown for PhaCYB4 from *B. cereus* YB-4, the involvement of Cys<sub>151</sub>, Asp<sub>306</sub>, and His<sub>335</sub> in  
158 polymerization activity was shown by site-directed mutagenesis [5].

159

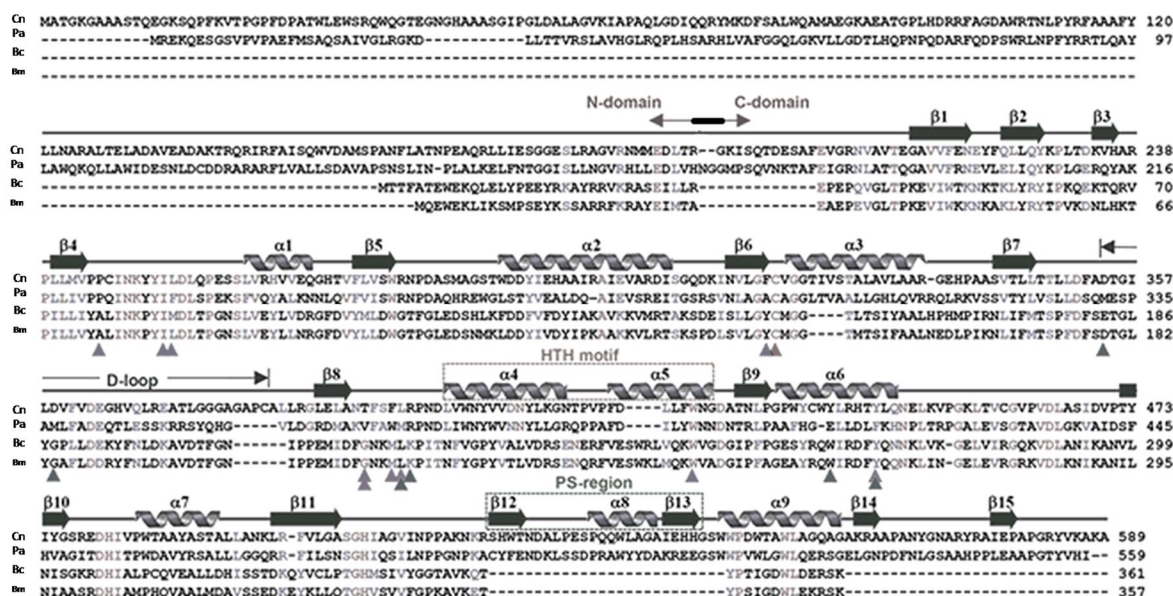
### 160 **Diversity and spread of phaC in bacteria**

161 PHA synthase genes can be identified in environmental bacterial strains for a preliminary screening,  
162 before knowledge on PHA synthesis ability due to the presence of the gene, using PCR amplification  
163 with conserved primers [7, 29]. Through PCR analyses, *phaC* genes were detected in a collection of  
164 bacterial strains isolated from soils and from marine environments. In samples of environmental  
165 strains, we amplified phaC gene sequences in colonies from environmental isolates, and performed  
166 DNA sequencing of ribosomal DNA to identify the strains at species level (unpublished results):  
167 with this method several species were classified for ability to produce PHA, namely *P. oleovorans*, *P.*  
168 *fluorescens*, *P. sihuiensis*, *P. putida*, *Comamonas testosteroni*, *Aeromonas hydrophila*, as well as *Cupriavidus*  
169 *necator*. It is envisaged that PCR screening using various different primer sets can be optimized to  
170 find new phaC polymorphisms and potential novel PHA synthase sequences. Quelas reported the  
171 presence in *Bradyrhizobium japonicum* USDA110 of five polyhydroxyalkanoate (PHA) synthases  
172 (PhaC), distributed into four different PhaC classes [30], and characterized the requirements for two  
173 of the genes in legume nodules under various physiological conditions.

174

175





176

177

Figure 1. Amino acid sequence and secondary structure of *Cupriavidus necator* PhaC<sub>C</sub>, aligned with the PHA synthase of class II (*P. aeruginosa*), class IVm and class IVb, from *Bacillus megaterium* and *B. cereus*, respectively.

178

179

180

### Crystal structure

181

182

183

184

185

186

187

188

189

190

191

192

193

In two publications appeared almost contemporarily, two teams reported on the crystal structure of PhaC<sub>C</sub>-CAT, the catalytic domain of PhaC from *Cupriavidus necator* [18, 19, 24]. PhaC<sub>C</sub>-CAT was shown to dimerize, and to adopt a partially open form maintaining a narrow substrate access to the active site. PhaC<sub>C</sub> needs PhaM, the primer of PHA synthesis, to start and accelerate polymer synthesis, and this may be due to increased accessibility of 3HB-CoA substrate to the active site. Wittenborn obtained the crystal structure of PhaC<sub>C</sub>(C<sub>319</sub>A), a construct in which the active site cysteine (Cys<sub>319</sub>) was mutated to alanine to improve protein stability in the absence of detergent. During the crystallization, proteolysis of PhaC<sub>C</sub> occurred after the N-domain (R<sub>192</sub>), leading to the crystal structure of the C-domain: PhaC<sub>C</sub>-CAT is formed by two Core subdomains (G<sub>143</sub>-F<sub>352</sub>, L<sub>450</sub>-A<sub>589</sub>), flanking on both sides a Dimerization domain (A<sub>353</sub>-L<sub>549</sub>) containing the dimerization loop (D-loop) and the Helix-loop-helix (HTH) domain; in addition, in the terminal Core sub-domain there is an Extended C-terminal region (EC: R<sub>521</sub>-A<sub>589</sub>), that is missing in class IV PhaC (figure 1), and a Protruding Structure, PS, that elongates from the Extended C-region.

194

195

196

197

198

199

200

201

202

203

The catalytic domain of PhaC<sub>C</sub> contains the residues 201–368 and 378–589 (with residues 369–377 devoid of any structure), showing an  $\alpha/\beta$ -hydrolase fold, featuring a central mixed  $\beta$ -sheet flanked by  $\alpha$ -helices on both sides. This architecture is similar to that seen in lipases. The CAT domain in the PhaC<sub>C</sub> sequence is structured by the presence of the  $\beta$ 1-4 sheets, the  $\alpha$ 1 helix, the  $\beta$ 5 sheet,  $\alpha$ 2 helix,  $\beta$ 6 sheet facing the lipase box, followed by the  $\alpha$ 3- $\beta$ 7 fold: after this structure there is the D-loop; after the  $\beta$ 8 sheet, there is the helix-loop-helix (HTH), composed of the  $\alpha$ 4 and  $\alpha$ 5 helices facing each other, and the  $\beta$ 9- $\alpha$ 6 fold, where the Dimerization subdomain ends (L<sub>449</sub>); as for the other amino acids of the catalytic triad, the aspartate is located between the  $\beta$ 10- $\alpha$ 7 fold, and the histidine is located after the  $\beta$ 11 sheet. The active site of PhaC<sub>C</sub> is accessible via a water-filled channel, with a size of 12.5 Angstrom, that can accommodate the 3HB-CoA substrate and/or short PHA oligomers.

204 Two PhaC monomers interact through the dimerization surfaces (A<sub>353</sub>-E<sub>445</sub>), containing hydrophobic  
205 amino acids, by means of interaction between one monomer helix-loop-helix motif (HTH) and the  
206 D-loop of the second monomer [18, 19].

207 In the report on the crystal structure obtained from the catalytic domain of PhaC from  
208 *Chromobacterium* sp. USM2, PhaC<sub>CS</sub>-CAT was compared to the PhaC<sub>CN</sub>-CAT crystal structure [17].  
209 Considering the two structures described, in PhaC<sub>CS</sub>-CAT a difference in the accessibility of the  
210 active site has been evidenced. Chek showed that in the PhaC<sub>CS</sub>-CAT dimer, the CAP and LID  
211 domains close the access to the substrate binding site [17]. The structure proposed by Chek and  
212 colleagues describing a PhaC<sub>CS</sub> active site covered by the CAP subdomain, differs from the partially  
213 open form of the PhaC<sub>CN</sub> catalytic domain reported by Wittenborn. The CAP domain occupies  
214 partially the access to the substrate binding pocket, and the LID domain needs to slide away in order  
215 to free the access for 3OH-alkanoyl-S-CoA units. Both catalytic domains of PhaC<sub>CS</sub> and PhaC<sub>CN</sub> form a  
216 dimer mediated by the CAP subdomain. The difference between the closed and partially open form  
217 is provided by the conformation of the CAP subdomain. The CAP subdomain undergoes a  
218 conformational change during catalytic activity with rearrangement of the dimeric form.

219 The main difference between the two crystal structures was found in the folding of  $\alpha B'$  and  $\eta B'$   
220 helices and their linker loop of PhaC<sub>CS</sub>-CAT, while the corresponding positions in PhaC<sub>CN</sub>-CAT,  
221 show a long  $\alpha 4$  helix that presents a partial access to the active site. The region Leu<sub>402</sub>-Asn<sub>415</sub>  
222 forming the  $\alpha 4$  helix in PhaC<sub>CN</sub>-CAT is conserved among Class I and II PHA synthases, whereas the  
223 corresponding segment, Leu<sub>369</sub>-Lys<sub>382</sub> of PhaC<sub>CS</sub>-CAT, displays a disordered structure.

224

### 225 **Catalytic mechanism**

226 The models proposed for the available PhaC structures, hypothesize the presence of a substrate  
227 entrance tunnel, that accommodates HB-CoA, with a size of about 12.5-13 Å, and a product egress  
228 tunnel, positioned perpendicularly to the entrance tunnel. Various catalytic mechanisms for PHA  
229 synthases have been proposed, in the context of dimerization of PHA synthases of class I and II [17].

230 One mechanism is referred to as the non-processive ping-pong model: this mechanism requires  
231 two cysteines in the active sites in the dimer, for PHA chain elongation, with chain transfer from one  
232 cysteine to the second active site. The ping-pong mechanism requires two thiol groups located at a  
233 distance short enough to shuttle back and forth the growing (3HB)<sub>n</sub> chain between the two thiols.  
234 The dimeric structures described by Wittenborn and by Kim for PhaC<sub>CN</sub>-CAT, and by Chek for  
235 PhaC<sub>CS</sub>, show that the two active sites are too distant (33 and 28.1 Angstrom, respectively) for  
236 successive chemical reactions.

237 The distance between the active sites in the dimer seems to favor the mechanism based on a  
238 single active site for each elongation reaction. In the model described by Chek, the dimer, composed  
239 by two units of phaC<sub>CS</sub> through the contacts between the two CAP domains and the two N-domains,  
240 presents two channels leading to the two active sites. The dimeric structure proposed by Chek [17],  
241 favors the involvement of one active site for each processing step. In the model, the substrate enters  
242 the substrate-binding tunnel, while chain product is elongated along a path near the protein surface,  
243 with a sliding mechanism of the PHA polymer under synthesis along a V shaped cavity within the  
244 enzyme. In the proposed structure, the enzyme moves along the extremity of the forming polymer to  
245 add new 3HB units, rather than hosting the polymer into a product egress channel. The mechanism  
246 involves a processive model that requires a single active site for PHA chain elongation and a  
247 non-covalent intermediate, in addition to a covalent intermediate bound to the Cys residue at the  
248 active center during the catalytic cycle. The enzyme dimer, through interactions with other partners,  
249 with substrate, phasins and phaM, move the CAP domains to flip away, opening the active site  
250 entrance, and freeing the product channel, and the two Core units contemporarily accept the  
251 substrate and produce the 3HB<sub>n</sub> polymers. The process occurs with a two step catalysis mechanism

252 that allows the intermediates to be located in the enlarged cavities partially freed from the CAP  
253 occupancy. The arrangement of the dimer, different from that of the PhaCC<sub>n</sub>-CAT dimer, may  
254 allow to the CAP subdomains to undergo a conformational change during catalytic activity with  
255 rearrangements in the dimer, that facilitate substrate entry, intermediate product formation, and  
256 product exit from the active site. According to the crystal structure of the PhaCC<sub>n</sub>-CAT dimer [18, 19]  
257 the substrates enter through the substrate-binding tunnel: the first 3HB-CoA is attacked by the  
258 nucleophilic Cys-SH to produce a 3HB-Cys covalent bond, as in the aforementioned model, and  
259 frees CoA-SH, that is released from the product egress tunnel. A second 3HB-CoA attacks 3HB-Cys  
260 thioester bond with the hydroxyl group in 3HB to produce a (3HB)<sub>2</sub>-CoA intermediate, reaction that  
261 frees the Cys residue in the active center. The Cys residue again attacks the thioester bond of the  
262 (3HB)<sub>2</sub>-CoA intermediate to produce (3HB)<sub>n+1</sub>, covalently bound to the Cys residue and release of  
263 free CoA. In this model, the growing 3HB polymer is bound to the enzyme at the end of each cycle.  
264 This model cannot allow to position large molecules such as (3HB)<sub>n</sub>-CoA intermediate within the  
265 substrate binding site, that has a cavity of 12.5 Angstrom.

266 An alternative model has been proposed with a succession of reactions slightly different. The  
267 model proposed for PhaCC<sub>n</sub>, by Wittenborn, implies that newly entered 3HB-CoA produces  
268 3HB-Cys; then (3HB)<sub>2</sub>-CoA enters the active site to produce (3HB)<sub>3</sub>-CoA, which is again released  
269 from the active site. When a new (3HB)<sub>2</sub>-CoA substrate binds, the HB hydroxyl group is  
270 deprotonated by His<sub>508</sub>, facilitated through modulation of the histidine basicity by Asp<sub>480</sub>. The newly  
271 formed HB alkoxide attacks the Cys-HB thioester, generating a noncovalent, CoA-bound  
272 intermediate. However, if the (3HB)<sub>3</sub>-CoA produced is held in the active site and attacked by the  
273 active Cys residue again to produce (3HB)<sub>3</sub>-Cys, chain elongation would then require an  
274 inter-subunit reaction. Again, (3HB)<sub>n</sub>-Cys adducts would require a larger active site cavity.

275

#### 276 **Mutation and amino acid substitution studies**

277 Several studies focused on PHB synthases with mutations enabling the enzymes to accelerate the  
278 reaction kinetics [31-33] and ability to accept bulk substrates as precursors for the production of  
279 mcl-PHAs and grafted copolymers.

280 Nomura and Taguchi [34] reviewed the attempts to engineer various classes of PHA synthases,  
281 either by mutagenesis or by evolution, in class I and Class II enzymes. The methods utilized either  
282 random mutagenesis, intragenic suppression mutagenesis, gene shuffling, random mutagenesis  
283 combined with Site-specific saturation mutagenesis and recombination, localized semi-random  
284 mutagenesis, PCR-mediated random chimeragenesis, intragenic suppression mutagenesis,  
285 site-specific saturation mutagenesis.

286 Many authors described mutations in amino acids positioned in various domains of different PHA  
287 synthases, most often finding a decrease in production of mcl-PHA and higher synthesis of scl-PHA.  
288 Beneficial effects of mutagenesis studies of Glu<sub>130</sub> and Ser<sub>477</sub> have been described [35-37]. For  
289 instance, the E<sub>130</sub>D substitution and S<sub>477</sub>X mutation in type II PHA synthase showed an  
290 enhancement of PHA production and alteration of polymer molecular weight.

291 A mutational study of PhaCC<sub>s</sub> reported by Chuah [40], showed that in PhaCC<sub>s</sub> Ala<sub>479</sub> is a critical  
292 residue required for substrate specificity, as determined by various site-specific mutational assays  
293 both *in vivo* and *in vitro*, and production tests of copolymers such as P(3HB-co-3HHx). In PhaCC<sub>n</sub> and  
294 in other Class I enzymes this position corresponds to the conserved residue Ala<sub>517</sub>. In the structure  
295 proposed by Chek, Ala<sub>479</sub> is located within  $\alpha 5$  helix and the side chain protrudes into a depression of  
296 the molecular surface formed by loops ( $\beta 4$ - $\alpha 1$ ,  $\beta 9$ - $\alpha 5$  and  $\alpha 5$ - $\beta 10$  loops) from the core subdomain,  
297 and is partially covered by the helix  $\eta B'$  and the following loop of the LID region from the CAP  
298 subdomain: the A<sub>479</sub> mutation results in weakening of the interactions between the LID region and  
299 the core subdomain, and stabilizes the active form of this enzyme by releasing the LID region from

300 the active site. Since Ala<sub>479</sub> is surrounded by polar residues (Ser<sub>475</sub> and Arg<sub>490</sub>), it is supposed that  
301 replacement of Ala<sub>479</sub> with Ser or Thr facilitates hydrogen-bonding interactions with the polar  
302 residues and stabilization of  $\alpha 5$  helix harboring the active residue His<sub>477</sub>, important for enzyme  
303 activity.

304 A mutagenesis study of class I PHA synthases showed that the F<sub>420</sub>S mutation in PhaC<sub>C<sub>1</sub></sub>  
305 increased the specific activity with a shortened lag phase [41]. This residue corresponds to Phe<sub>387</sub> of  
306 PhaC<sub>C<sub>s</sub></sub>, which is conserved among Class I and II PHA synthases, and is located in  $\alpha C$  helix of the  
307 CAP domain. Phe<sub>387</sub> is involved in dimerization by participating in an intermolecular nonpolar  
308 interaction linking the  $\alpha C$  helix to the LID region, suggesting that the mutation may affect the  
309 conformational stability and/or conformation transition of the LID region.

310 The CAP subdomain provides  $\alpha C$  and  $\alpha D$  helices as building blocks of the active site cavity filled  
311 with a cluster of water molecules. In the structure obtained by Chek [17], the C-terminal portion of  
312 the LID region of the CAP subdomain is disordered and is followed by  $\alpha C$  helix docked to the core  
313 subdomain. Two highly conserved residues, Trp<sub>392</sub> and Asp<sub>395</sub>, are present in  $\alpha C$  helix. Trp<sub>392</sub> of  
314 PhaC<sub>C<sub>s</sub></sub> is located in the  $\alpha C$  helix of the CAP subdomain and faces Site B of the channel.

315 Amara and Rhem attempted to modify the activity of PhaC from *Pseudomonas* species [37]. The  
316 conserved residue Trp<sub>398</sub> was replaced, such as Trp<sub>398</sub>Phe and Trp<sub>398</sub>Ala, and the mutation resulted  
317 in inactivation of the enzyme. Using the threading model of enzyme structure, the authors located  
318 the Trp residue as exposed on the surface, in agreement with the results shown by Chek for class I  
319 enzymes [42-46].

320 Tyr<sub>412</sub> in PhaC<sub>C<sub>s</sub></sub>, and Tyr<sub>446</sub> in the  $\alpha 6$  helix in PhaC<sub>C<sub>1</sub></sub>, are residues conserved in Class I, III and IV  
321 PHA synthases, while Phe occupies this position in Class II synthases: in addition to this amino acid  
322 position, there is a second substitution that seems to have a role in accommodating larger substrates.  
323 Tyr<sub>438</sub> is conserved in Class I, III and IV enzymes, while in Class II PhaC this position is occupied by  
324 His: this may contribute to a reduction of size, eliminating the bulky side chain (phenol ring), and  
325 determining changes in polar interactions with other amino acids facing the substrate entrance  
326 tunnel; these amino acids interactions may account for the property to accommodate large substrates  
327 in class II enzymes.

328 PhaC<sub>1</sub> and PhaC<sub>2</sub> from *Pseudomonas stutzeri* [39], have been applied to produce mcl-PHAs in  
329 engineered bacteria. *Ps*PhaC<sub>2</sub> with four point mutations, at E<sub>130</sub>D, S<sub>325</sub>T, S<sub>477</sub>G, and Q<sub>481</sub>K was used to  
330 accommodate substrates with various shapes and structures, to produce mcl-PHAs and block  
331 copolymers. The putative catalytic residues Cys<sub>296</sub>, Asp<sub>452</sub>, His<sub>453</sub> and His<sub>480</sub> were replaced by  
332 site-specific mutagenesis [37]. Considering the *Pseudomonas* mcl-PHA synthases, the His<sub>480</sub>Gln  
333 substitution did not affect enzyme activity, posing the doubt that His is not a component of the  
334 catalytic triad. As for a second conserved histidine, when His<sub>453</sub> was replaced by Gln, the modified  
335 enzyme showed only 24% of wild-type in vivo activity, which make suppose that His<sub>453</sub> might be  
336 part of the catalytic triad in class II PHA synthases [37]. However, no other study confirmed the  
337 involvement of His<sub>453</sub> in class II PhaC<sub>2</sub> catalysis.

338 Sheu studied the increase of PHA synthase thermostability and activity, using chimeric  
339 constructs, indicating that some amino acid substitutions may stabilize the enzyme at higher  
340 temperature [31].

341

#### 342 **Production of PHA in fermentors**

343 Various companies are involved in production of bioplastics for industrial applications. The  
344 methods are various, either using patented strains, engineered PHA synthases, and growth  
345 conditions favoring the high yield and high PHA content/dry cell weight. In the field of monitoring



346 the endpoint step of PHA synthesis, and bacteria collection, various methods have been established,  
347 from lipid staining [47] and analysis of fluorescence intensity, to physic-chemical analyses (Raman,  
348 FTIR spectra). Since bacterial cultures require sterilization that is costly at industrial scale, methods  
349 based on halophilic strains have been proposed as to circumvent the sterilization process. Extraction  
350 of PHAs from bacteria requires costly procedures, therefore researchers used Archea or  
351 cyanobacteria that have PHA granules easily extracted, decreasing the costs of production.

352

### 353 **Progress and advancements in PHA field**

354 Recent advancements on PHA granule structure and composition have been achieved [48].  
355 The high molecular weight storage PHB consists of  $> 10^3$  3HB residues (storage PHB). PHB granules  
356 *in vivo* are covered by a surface layer that is distinct from the polymer core. PHA granules are  
357 structured through the action of various proteins on the surface. The granules, named also  
358 carbonosomes, represent supramolecular complexes with specific functions. In addition to Phasins  
359 (such as PhaP2, PhaP3, PhaP4), among the proteins identified during PHA granule isolation, there  
360 are the PHB synthase (PhaC1), PhaM, the activator of PhaC, Acetyl-CoA acetyltransferase, and  
361 acylCoA synthetase: their presence may be explained by the need to avoid accumulation of CoA-SH,  
362 produced by the PHA synthase during polymer synthesis, since an excess of CoA would inhibit the  
363 enzyme. The most accurate model for PHA synthesis within bacterial cell is the Scaffold Model: it  
364 assumes that PHB synthase of nascent PHB granules is attached to a scaffold within the cell. PHB  
365 granules have been localized in the cell centre, along with the length axis of the bacteria. PhaM, that  
366 specifically interacts with PhaC1 and with phasin PhaP5, interacts also with DNA and with the  
367 nucleoid *in vitro* and *in vivo*, and this may explain why PHB granules have been found attached to  
368 the bacterial nucleoid.

372

373

374

### 374 **Conclusions**

375 In this review, we reported on the classification of PHA synthases, the proposed structures and role  
376 of individual amino acids in the catalysis and mechanism of activity of class I and class II PHA  
377 synthases, presenting the information available on the other types of enzymes. We have reviewed  
378 the engineering attempts and the effect of modification of key amino acids on the enzymatic activity  
379 and product formation. It is expected that PHA synthases may be further improved to produce  
380 effectively and at convenient costs tailor-made polymers.

381

382 **Acknowledgments:** No funds have been provided for covering the costs to publish in open access.

383 **Author Contributions:** V.M. and O.F.D. provided the information on research data on environmental strains.  
384 P.P. wrote and reviewed the manuscript.

385 **Conflicts of Interest:** "The authors declare no conflict of interest."

### 386 **References**

- 387 1. Kumar P, Jun HB, Kim BS. Co-production of polyhydroxyalkanoates and carotenoids through  
388 bioconversion of glycerol by *Paracoccus* sp. strain LL1. *Int J Biol Macromol.* **2018**; *107*, 2552-2558. doi:  
389 10.1016/j.ijbiomac.2017.10.147
- 390 2. Park, D.H., and Kim, B.S. Production of poly(3-hydroxybutyrate) and  
391 poly(3-hydroxybutyrate-co-4-hydroxybutyrate) by *Ralstonia eutropha* from soybean oil. *New Biotechnol.*  
392 **2011**; *28*, 719-24. doi: 10.1016/j.nbt.2011.01.007.
- 393 3. Kumar, P., Singh, M., Mehariya, S., Patel, S.K., Lee, J.K., Kalia, V.C. Ecobiotechnological approach for  
394 exploiting the abilities of *Bacillus* to produce co-polymer of Polyhydroxyalkanoate. *Indian J Microbiol.*  
395 **2014**, *54*, 151-7. Doi: 10.1007/s12088-014-0457-9
- 396 4. Hermann-Krauss, C., Koller, M., Muhr, A., Fas, H., Stelzer, F., Braunegg, G. Archaeal production of  
397 polyhydroxyalkanoate (PHA) co- and terpolyesters from biodiesel industry-derived by-products.  
398 *Archaea* **2013**, 129268. Doi: 10.1155/2013/129268

- 399 5. Tsuge, T., Hyakutake, M., Mizuno, K. Class IV polyhydroxyalkanoate (PHA) synthases and  
400 PHA-producing *Bacillus*. *Appl Microbiol Biotechnol.* **2015**, *99*, 6231-40. doi: 10.1007/s00253-015-6777-9
- 401 6. Ansari, S., and Fatma, T. Cyanobacterial polyhydroxybutyrate (PHB): Screening, optimization and  
402 characterization. *PLoS One* **2016**; *11*, e0158168. Doi: 10.1371/journal.pone.0158168
- 403 7. Tan G-Y.A., Chen, C.-L., Li, L., Ge, L., Wang, L., Ningtyas Razaad, I.M., Li, Y., Zhao, L., Mo, Y., Wang,  
404 J.-Y. Start a research on biopolymer polyhydroxyalkanoate (PHA): A review. *Polymers* (Basel) **2014**, *6*,  
405 706-754. Doi: 10.3390/polym6030706
- 406 8. Poltronieri, P., Mezzolla, V.; D'Urso, O.F. PHB production in biofermentors assisted through biosensor  
407 applications. *Proceedings* (Basel), 2017, *1*, 4. Doi:10.3390/ecs3-3-E014
- 408 9. Chen, G.-Q., Hajnal, I., Wu, H., Lv, L., Ye, J. Engineering biosynthesis mechanisms for diversifying  
409 Polyhydroxyalkanoates. *Trends Biotechnol.* 2015, *33*:565-574, doi: 10.1016/j.tibtech.2015.07.007 565
- 410 10. Chen, G.-Q., and Hajnal, I. The 'PHAome'. *Trends Biotechnol.* **2015**, *33*, 559-564. Doi:  
411 10.1016/j.tibtech.2015.07.006
- 412 11. Le Meur, S., Zinn, M., Egli, T., Thöny-Meyer, L., Ren, Q. Production of medium-chain-length  
413 polyhydroxyalkanoates by sequential feeding of xylose and octanoic acid in engineered *Pseudomonas*  
414 *putida* KT2440. *BMC Biotechnol.* **2012**, *12*, 53. Doi: 10.1186/1472-6750-12-53.
- 415 12. Anjum, A., Zuber, M., Zia, K.M., Noreen, A., Anjum, M.N., Tabasum, S. Microbial production of  
416 polyhydroxyalkanoates (PHAs) and its copolymers: a review of recent advancements. *Int J Biol*  
417 *Macromol* **2016**, *89*, 161-174.
- 418 13. Meng, D.C., Shen, R., Yao, H., Chen, J.C., Wu, Q., Chen, G.Q. Engineering the diversity of polyesters.  
419 *Curr Opin Biotechnol.* **2014**; *29*, 24-33. Doi: 10.1016/j.copbio.2014.02.013.
- 420 14. Mezzolla, V; D'Urso, OF, Poltronieri, P. Optimization of polyhydroxyalkanoate production by  
421 recombinant *E. coli* supplemented with different plant by-products. *Biotechnol Indian J.* **2017**, *13*, 138.
- 422 15. Zhang, W., Chen, C., Cao, R., Maurmann, L., Li, P. Inhibitors of polyhydroxyalkanoate (PHA)  
423 synthases: synthesis, molecular docking, and implications. *Chembiochem.* **2015**, *16*, 156-166. Doi:  
424 10.1002/cbic.201402380
- 425 16. Bhubalan, K., Chuah, J.A., Shozui, F., Brigham, C.J., Taguchi, S., Sinskey, A.J., Rha, C., Sudesh, K.  
426 Characterization of the highly active polyhydroxyalkanoate synthase of *Chromobacterium* sp. strain  
427 USM2. *Appl Environ Microbiol.* **2011**, *77*, 2926-2933.
- 428 17. Chek, M.F., Kim, S.Y., Mori, T., Arsad, H., Samian, M.R., Sudesh, K., Hakoshima, T. Structure of  
429 polyhydroxyalkanoate (PHA) synthase PhaC from *Chromobacterium* sp. USM2, producing  
430 biodegradable plastics. *Sci Rep.* **2017**, *7*, 5312. DOI: 10.1038/s41598-017-05509-4
- 431 18. Wittenborn, E.C., Jost, M., Wei, Y., Stubbe, J., Drennan, C.L. Structure of the Catalytic Domain of the  
432 Class I Polyhydroxybutyrate Synthase from *Cupriavidus necator*. *J. Biol. Chem* **2016**, *291*, 25264-25277.
- 433 19. Kim, J., Kim, Y.-J., Choi, S. Y., Lee, S. Y. & Kim, K.-J. Crystal structure of *Ralstonia eutropha*  
434 polyhydroxyalkanoate synthase C-terminal domain and reaction mechanisms. *Biotechnol. J* **2017**, *12*,  
435 1600648. DOI: 10.1002/biot.201600648
- 436 20. Kumar, P., Ray, S., Kalia, V.C. Production of co-polymers of polyhydroxyalkanoates by regulating the  
437 hydrolysis of biowastes. *Bioresource Technol.* **2016**, *200*, 413-419. doi: 10.1016/j.biortech.2015.10.045
- 438 21. Zou, H., Shi, M., Zhang, T., Li, L., Li, L., Xian, M. Natural and engineered polyhydroxyalkanoate  
439 (PHA) synthase: key enzyme in biopolyester production. *Appl Microbiol Biotechnol.* **2017**, *101*,  
440 7417-7426. DOI: 10.1007/s00253-017-8485-0
- 441 22. Kihara, T., Hiroe, A., Ishii-Hyakutake, M., Mizuno, K., Tsuge, T. *Bacillus cereus*-type  
442 polyhydroxyalkanoate biosynthetic gene cluster contains R-specific enoyl-CoA hydratase gene. *Biosci*  
443 *Biotechnol Biochem.* **2017**, *81*, 1627-1635. doi: 10.1080/09168451.2017.1325314.
- 444 23. Hyakutake M, Tomizawa S, Mizuno K, Abe H, Tsuge T. Alcoholic cleavage of  
445 polyhydroxyalkanoate chains by class IV synthases induced by endogenous and exogenous ethanol.  
446 *Appl Environ Microbiol.* **2014**; *80*, 1421-9. doi: 10.1128/AEM.03576-13

- 447 24. Kim, Y.-J., Choi, S.Y., Kim, J., Jin, K.S., Lee, S.Y., Kim, K.-J. Structure and function of the N-terminal  
448 domain of *Ralstonia eutropha* polyhydroxyalkanoate synthase, and the proposed structure and  
449 mechanisms of the whole enzyme. *Biotechnol. J.* **2017**, *12*, 1600649. DOI: 10.1002/biot.201600649
- 450 25. Tsuge, T., Imazu, S., Takase, K., Taguchi, S., Doi, Y. An extra large insertion in the  
451 polyhydroxyalkanoate synthase from *Delftia acidovorans* DS-17: its deletion effects and relation to  
452 cellular proteolysis. *FEMS Microbiology Letters* **2004**, *231*, 77-83. Doi: 10.1016/S0378-1097(03)00930-3
- 453 26. Qi, Q., and Rehm, B.H. Polyhydroxybutyrate biosynthesis in *Caulobacter crescentus*: molecular  
454 characterization of the polyhydroxybutyrate synthase. *Microbiology* **2001**, *147*, 3353-8.
- 455 27. Ilham, M., Nakanomori, S., Kihara, T., Hokamura, A., Matsusaki, H., Tsuge, T., Mizuno, K.  
456 Characterization of polyhydroxyalkanoate synthases from *Halomonas* sp. O-1 and *Halomonas elongata*  
457 DSM2581: Site-directed mutagenesis and recombinant expression. *Polymer Degrad. Stability* **2014**, *109*,  
458 416-423. Doi: 10.1016/j.polymdegradstab.2014.04.024
- 459 28. Chen, J.-Y., Song, G., Chen, G.-Q. A lower specificity PhaC2 synthase from *Pseudomonas stutzeri*  
460 catalyses the production of copolyesters consisting of short-chain-length and medium-chain-length  
461 3-hydroxyalkanoates. *Antonie van Leeuwenhoek* **2006**, *89*, 157-167. Doi: 10.1007/s10482-005-9019-9
- 462 29. Montenegro, E.M.D.S., Delabary, G.S., Silva, M.A.C.D., Andreote, F.D., Lima, A.O.S. Molecular  
463 diagnostic for prospecting polyhydroxyalkanoate-producing bacteria. *Bioengineering* (Basel) **2017**; *4*, 52.  
464 Doi: 10.3390/bioengineering4020052.
- 465 30. Quelas, J.I., Mongiardini, E.J., Pérez-Giménez, J., Parisi, G., Lodeiro, A.R. Analysis of two  
466 polyhydroxyalkanoate synthases in *Bradyrhizobium japonicum* USDA 110. *J. Bacteriol.* **2013**, *195*, 3145-55.  
467 Doi: 10.1128/JB.02203-12.
- 468 31. Sheu, D.S., Chen, W.M., Lai, Y.W., Chang, R.C. Mutations derived from the thermophilic  
469 polyhydroxyalkanoate synthase PhaC enhance the thermostability and activity of PhaC from  
470 *Cupriavidus necator* H16. *J. Bacteriol.* **2012**, *194*, 2620-2629. Doi: 10.1128/JB.06543-11
- 471 32. Takase, K., Matsumoto, K., Taguchi, S., Doi, Y. Alteration of substrate chain-length specificity of type II  
472 synthase for polyhydroxyalkanoate biosynthesis by *in vitro* evolution: *in vivo* and *in vitro* enzyme  
473 assays. *Biomacromolecules* **2004**, *5*, 480-485. Doi: 10.1021/bm034323+
- 474 33. Chen, C., Cao, R., Shrestha, R., Ward, C., Katz, B.B., Fischer, C.J., Tomich, J.M., Li P. Trapping of  
475 intermediates with substrate analog HBOCoA in the polymerizations catalyzed by class III  
476 polyhydroxybutyrate (PHB) synthase from *Allochromatium vinosum*. *ACS Chem Biol.* **2015**, *10*,  
477 1330-1339. Doi: 10.1021/cb5009958.
- 478 34. Nomura, C.T., and Taguchi, S. PHA synthase engineering toward superbio-catalysts for custom-made  
479 biopolymers. *Applied Microbiol Biotechnol.* **2007**, *73*, 969-979. DOI: 10.1007/s00253-006-0566-4
- 480 35. Matsumoto, K., Takase, K., Aoki, E., Doi, Y., Taguchi, S. Synergistic effects of Glu130Asp substitution  
481 in the type II polyhydroxyalkanoate (PHA) synthase: enhancement of PHA production and alteration  
482 of polymer molecular weight. *Biomacromolecules* **2005**, *6*, 99-104.
- 483 36. Matsumoto, K., Aoki, E., Takase, K., Doi, Y., Taguchi, S. In vivo and in vitro characterization of  
484 Ser477X mutations in polyhydroxyalkanoate (PHA) synthase 1 from *Pseudomonas* sp. 61-3: effects of  
485 beneficial mutations on enzymatic activity, substrate specificity, and molecular weight of PHA.  
486 *Biomacromolecules* **2006**, *7*, 2436-2442.
- 487 37. Amara, A.A., and Rehm, B.H. Replacement of the catalytic nucleophile cysteine-296 by serine in class II  
488 polyhydroxyalkanoate synthase from *Pseudomonas aeruginosa*-mediated synthesis of a new polyester:  
489 identification of catalytic residues. *Biochem. J.* **2003**, *374*, 413-21.
- 490 38. Zou, H., Shi, M., Zhang, T., Li, L., Li, L., Xian, M. Natural and engineered polyhydroxyalkanoate  
491 (PHA) synthase: key enzyme in biopolyester production. *Appl. Microbiol. Biotechnol.* **2017**; *101*,  
492 7417-7426. doi: 10.1007/s00253-017-8485-0.
- 493 39. Chen, J.-Y., Liu, T., Zheng, Z., Chen, J.C., Chen, G.-Q. Polyhydroxyalkanoate synthases PhaC1 and  
494 PhaC2 from *Pseudomonas stutzeri* 1317 had different substrate specificities. *FEMS Microbiol Lett* **2004**,  
495 *234*, 231-237. Doi: 10.1016/j.femsle.2004.03.029
- 496 40. Chuah, J.A., Tomizawa, S., Yamada, M., Tsuge, T., Doi, Y., Sudesh, K., Numata, K. Characterization of  
497 site-specific mutations in a short-chain-length/medium-chain-length polyhydroxyalkanoate synthase:  
498 *In vivo* and *in vitro* studies of enzymatic activity and substrate specificity. *Appl. Environ. Microbiol.* **2013**,  
499 *79*, 3813-3821. Doi: 10.1128/AEM.00564-13

- 500 41. Normi, Y.M., Hiraishi, T., Taguchi, S., Sudesh, K., Najimudin, N., Doi, Y. Site-directed saturation  
501 mutagenesis at residue F420 and recombination with another beneficial mutation of *Ralstonia eutropha*  
502 polyhydroxyalkanoate synthase. *Biotechnol. Lett.* **2005**, *27*, 705–712.
- 503 42. Tsuge, T., Saito, Y., Kikkawa, Y., Hiraishi, T., Doi, Y. Biosynthesis and compositional regulation of  
504 poly(3-hydroxybutyrate)-co-(3-hydroxyhexanoate) in recombinant *Ralstonia eutropha* expressing  
505 mutated polyhydroxyalkanoate synthase genes. *Macromol Biosci.* **2004**, *4*, 238–242. DOI:  
506 10.1002/mabi.200300077
- 507 43. Shozui, F., Matsumoto, K., Sasaki, T., Taguchi, S. Engineering of polyhydroxyalkanoate synthase by  
508 Ser477X/Gln481X saturation mutagenesis for efficient production of 3-hydroxybutyrate-based  
509 copolyesters. *Appl Microbiol Biotechnol.* **2009**, *84*, 1117–1124. Doi: 10.1007/s00253-009-2052-2
- 510 44. Tsuge, T., Watanabe, S., Shimada, D., Abe, H., Doi, Y., Taguchi, S. Combination of N149S and D171G  
511 mutations in *Aeromonas caviae* polyhydroxyalkanoate synthase and impacton polyhydroxyalkanoate  
512 biosynthesis. *FEMS Microbiol Lett.* **2007**, *277*, 217–222. Doi: 10.1111/j.1574-6968.2007.00958.x
- 513 45. Gao, X., Yuan, X.X., Shi, Z.Y., Guo, Y.Y., Shen, X.W., Chen, J.C., Wu, Q., Chen, G.-Q. Production of  
514 copolyesters of 3-hydroxybutyrate and medium-chain-length 3-hydroxyalkanoates by *E. coli*  
515 containing an optimized PHA synthase gene. *Microb Cell Factories* **2012**, *11*, 130. Doi:  
516 10.1186/1475-2859-11-130
- 517 46. Shen, X.W., Shi, Z.Y., Song, G., Li, Z.J., Chen, G.-Q. Engineering of polyhydroxyalkanoate (PHA)  
518 synthase PhaC2Ps of *Pseudomonas stutzeri* via site-specific mutation for efficient production of PHA  
519 copolymers. *Appl Microbiol Biotechnol.* **2011**, *91*, 655–665. Doi: 10.1007/s00253-011-3274-7
- 520 47. Choi, J.E., Na, H.Y., Yang, T.H., Rhee, S.K., Song, J.K. A lipophilic fluorescent LipidGreen1-based  
521 quantification method for high-throughput screening analysis of intracellular poly-3-hydroxybutyrate.  
522 *AMB Express* **2015**, *5*, 131. doi: 10.1186/s13568-015-0131-6
- 523 48. Jendrossek, D., and Pfeiffer, D. New insights in the formation of polyhydroxyalkanoate granules  
524 (carbonosomes) and novel functions of poly(3-hydroxybutyrate). *Environ Microbiol.* **2014**, *16*, 2357-73.  
525 doi: 10.1111/1462-2920.12356  
526